Applied Physics Letters

Demonstration of GaN-based metal–insulator–semiconductor junction by hydrogen plasma treatment

Cite as: Appl. Phys. Lett. **117**, 052105 (2020); https://doi.org/10.1063/5.0018473
Submitted: 15 June 2020 . Accepted: 24 July 2020 . Published Online: 06 August 2020

Chen Yang, Houqiang Fu, Po-Yi Su, Hanxiao Liu, Kai Fu, Xuanqi Huang, Tsung-Han Yang, Hong Chen, Jingan Zhou, Xuguang Deng, Jossue Montes, Xin Qi, Fernando A. Ponce, and Yuji Zhao

Applied Physics Letters ARTICLE scitation.org/journal/apl

Demonstration of GaN-based metal–insulator–semiconductor junction by hydrogen plasma treatment

Cite as: Appl. Phys. Lett. **117**, 052105 (2020); doi: 10.1063/5.0018473
Submitted: 15 June 2020 · Accepted: 24 July 2020 ·
Published Online: 6 August 2020

View Online Export Citation CrossMark

Chen Yang,[1] Houqiang Fu,[1] Po-Yi Su,[2] Hanxiao Liu,[2] Kai Fu,[1] Xuanqi Huang,[1] Tsung-Han Yang,[1] Hong Chen,[1] Jingan Zhou,[1] Xuguang Deng,[1] Jossue Montes,[1] Xin Qi,[1] Fernando A. Ponce,[2] and Yuji Zhao[1,a)]

AFFILIATIONS

[1]School of Electrical, Computer and Energy Engineering, Arizona State University, Tempe, Arizona 85287, USA
[2]Department of Physics, Arizona State University, Tempe, Arizona 85287, USA

[a)]Author to whom correspondence should be addressed: yuji.zhao@asu.edu

ABSTRACT

We demonstrate a nickel/insulating-GaN (*i*-GaN)/*p*-type GaN junction and investigate its electrical properties. The *i*-GaN is formed by exposure to a low-power hydrogen plasma to passivate the *p*-GaN layer. Cathodoluminescence spectroscopy of the *i*-GaN is used to understand the passivation effect of the hydrogen plasma on *p*-GaN. The junction shows very low leakage ($<10^{-9}$ A at -50 V), excellent rectifying properties ($\sim 10^7$), high temperature stability, and blue light electroluminescence at forward bias. A bandgap model is proposed to illustrate the electrical properties of hydrogenated *p*-GaN and to understand the device characteristics.

III-nitrides including (Al, Ga, In)N and their alloys have shown great potential in optoelectronics,[1] photonics,[2] and electronics.[3] Recently, GaN electronic devices have been extensively studied due to GaN's wide bandgap (*Eg*), high breakdown electric field (E_b), and large Baliga's figure of merit (BFOM). Magnesium doped *p*-type GaN is critical for GaN electronic devices such as vertical p–n junctions, normally off high-electron-mobility transistors (HEMTs),[4] and junction field-effect transistors.[5] Hydrogen plays an important role in metal organic chemical vapor deposition (MOCVD) of *p*-type GaN films. H_2 is usually used as a carrier gas; however, H can also passivate Mg acceptors by forming neutral Mg–H complexes, rendering Mg-doped GaN high resistance ($>10^6$ Ω cm).[6] High temperature annealing in a non-hydrogen-containing atmosphere is a routine procedure to achieve high concentration of hole carriers in Mg-doped *p*-GaN.[7]

Hydrogen can also be intentionally introduced by exposure to hydrogen plasma to selectively passivate *p*-GaN.[8] Inductively coupled plasma (ICP) technology enables controlled hydrogen plasma treatment, which turns *p*-GaN into insulating GaN (*i*-GaN). Currently, the hydrogenated *p*-GaN or *i*-GaN has been mainly applied as a substitute for mesa etching to improve the device performance of GaN diodes and AlGaN/GaN HEMTs. Fu *et al.* reported the hydrogen-plasma-based edge termination technique for GaN vertical power *p–n* diodes.[9,10] The diodes showed superior performance compared with devices with mesa etching. Hydrogen-plasma based guard rings (GRs) have also been demonstrated, which can further improve the *p–n* diodes' performance.[11] Hao *et al.* reported hydrogen plasma treatment to realize normally off *p*-GaN/AlGaN/GaN HEMT devices,[12,13] where the hydrogen plasma passivates *p*-GaN to release electrons in the two-dimensional electron gas (2DEG) channel. In addition, the *i*-GaN can also increase gate control capability and reduce leakage current.

However, the understanding of the electrical properties of hydrogen-plasma-treated *p*-GaN is still not clear except for its high resistance. The optical properties and band structure of hydrogenated *p*-GaN are not well understood. Its applications have also been limited to supportive structures for device isolation and current blocking. In this work, we incorporate *i*-GaN as an insulator in a Ni/*i*-GaN/*p*-GaN metal–insulator–semiconductor (MIS) junction. This junction is different from previous reports of GaN MIS junctions with larger-bandgap dielectric materials (e.g., Fe_3O_4,[14] Y_2O_3,[15] Al_2O_3,[16] and Sm_2O_3[17]) as interlayers, which are usually very thin (<3 nm) allowing electrons to tunnel through. The *i*-GaN in the MIS junction behaves not only like an insulator but also like an intrinsic semiconductor allowing for minority carrier injections. The electrical characteristics of this junction indicate that the hydrogenated *p*-GaN still maintains a

single crystal structure with the Fermi level close to middle of the bandgap. This junction shows excellent rectifying behaviors, very low leakage, and high temperature stability. Furthermore, it also exhibits different electrical properties as compared to conventional p–n diodes and Schottky diodes.[18,19]

Two *p*-GaN epilayers were grown homoepitaxially on an n^+-GaN bulk substrate with an unintentionally doped GaN (*u*-GaN) buffer layer [Fig. 1(a)]. The two *p*-GaN epilayers are a 500-nm-thick *p*-GaN (Mg = 10^{19} cm^{-3}) and a 20-nm-thick heavily doped p^+-contact layer (Mg = 2×10^{20} cm^{-3}). Metal stacks of Pd/Ni/Au (20/30/100 nm) were deposited by electron beam evaporation. The Ohmic contacts were subsequently formed by annealing at 450 °C in nitrogen ambient by rapid thermal annealing (RTA) for 5 min. The *i*-GaN was formed by exposing *p*-GaN to low-power short-time hydrogen plasma generated by an inductively coupled plasma (ICP) system, with ICP power of 300 W and RF power of 5 W for 30 s [Fig. 1(b)]. The Ohmic contacts served as self-aligned masks to protect the *p*-GaN underneath. The samples were then treated by a 30-s 400 °C RTA to facilitate the formation of the Mg–H complexes. Finally, metal stacks of Ni/Au (20/100 nm) were deposited as contacts on plasma-treated *p*-GaN. The top view of a representative device is shown in Fig. 1(d).

Figure 2(a) is the cross-sectional secondary-electron (SE) image of the region near the edge of an Ohmic contact, obtained using an electron-beam accelerating voltage of 1.2 kV. Our previous work showed that under these conditions the untreated *p*-GaN film had a brighter contrast than the plasma-treated *p*-GaN film.[20] A clear boundary was observed between the plasma-treated and untreated *p*-GaN regions, indicating that only the top portion of the *p*-GaN film has been passivated. The film thickness of the plasma-treated and unaffected *p*-GaN was ~270 nm and ~250 nm, respectively. The passivation effect of the hydrogen plasma on *p*-GaN was studied by cathodoluminescence (CL) spectroscopy at room temperature. The CL measurements were carried out in a scanning electron microscope (SEM) at various electron acceleration voltages while keeping the same electron-beam current at 250 pA. By adjusting the acceleration voltage, we were able to probe the radiative recombination of *p*-GaN layers at various depths. The incident electron beams plunge into the *p*-GaN and stop at a certain depth that can be estimated by the following equation:[21]

$$R = 5.025 \times 10^{-12} A E_0^{1.67} \rho^{-1} Z^{-0.889} \lambda^{-1}, \quad (1)$$

where R (cm) is the maximum depth, A (g/mol) is the GaN molar mass, E_0 (V) is the accelerating voltage, Z is the Ga atomic number, ρ (g/cm^{-3}) is the density, and $\lambda = 0.182$ is a constant determined experimentally.[21] The acceleration voltages at 3 kV, 5 kV, and 7 kV corresponded to depths in *p*-GaN at ~113 nm, ~267 nm, and ~468 nm, respectively, as shown in the inset of Fig. 2(b). Figure 2(b) shows the CL spectra of plasma-treated *p*-GaN with different acceleration voltages. It should be noted that the incident electron beams did not penetrate the affected *p*-GaN with 3 kV and 5 kV acceleration voltages. Figure 2(c) illustrates different transition mechanisms[22–25] for the CL emission peaks in the spectra in Fig. 2(b). The 3.4 eV peak has been attributed to near-band edge excitonic transitions, the 3.25 eV peak corresponds to shallow-donor to Mg-acceptor transitions, and the 2.9 eV peak is related to deep-donor to Mg-acceptor transition. The origin of deep donor states may be complexes formed by nitrogen vacancies with the nearest neighbor Mg atoms (V_N-Mg_{Ga}).[22–24]

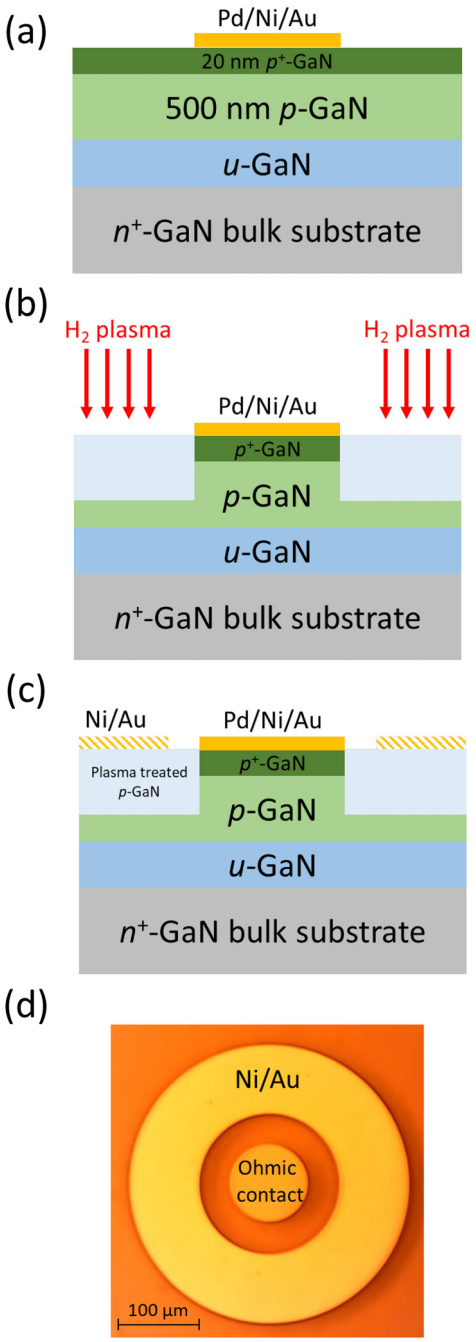

FIG. 1. MIS junction fabrication steps: (a) metal contact deposition, (b) RTA treatment and H_2 plasma passivation, (c) contact deposition on plasma-treated *p*-GaN, and (d) top view of device.

The luminescence characteristics of *p*-GaN are closely related to the Mg doping concentration.[26,27] For lightly doped *p*-GaN ([Mg] ≤ 1×10^{19} cm^{-3}), only the 3.4 and 3.25 eV peaks are observed in the luminescence spectrum. The 2.9 eV peak appears at sufficiently high Mg doping concentrations and becomes dominant in highly doped *p*-GaN

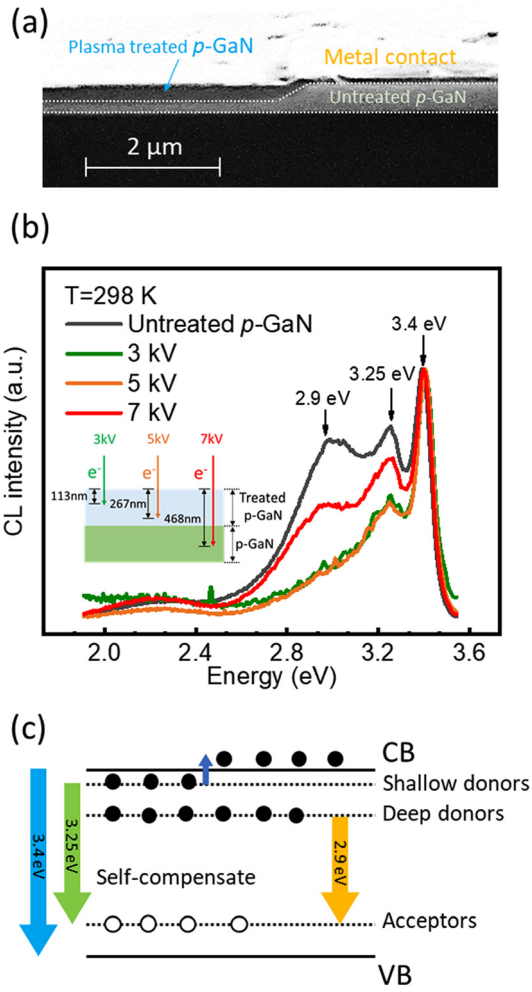

FIG. 2. (a) Cross section secondary-electron view at the edge of a metal contact. (b) CL depth profiling of H_2 plasma-treated GaN using increasing electron-beam accelerating voltages. The 7 kV spectrum probes the H_2-untreated *p*-GaN, used a reference. (c) Electronic states associated with the 2.9, 3.25, and 3.4 eV transitions in *p*-GaN.

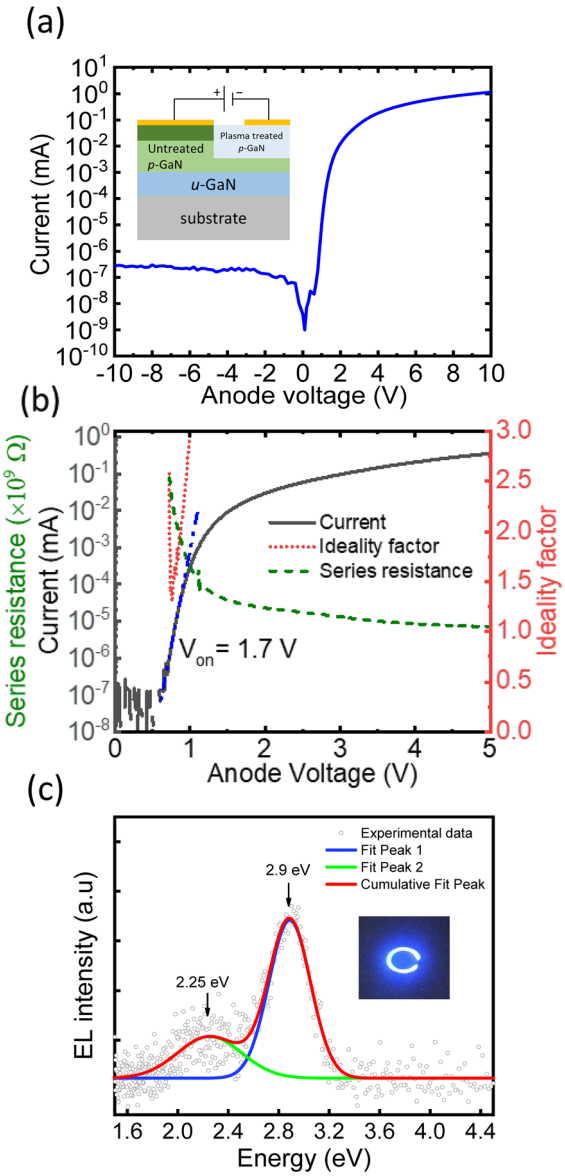

FIG. 3. Electrical properties of the MIS junction. (a) Rectifying characteristics in the range −10 V to 10 V. (b) Forward *I–V* characteristics at room temperature, also showing ideality factor and series resistance values. (c) EL spectrum and fittings with light emission shown in the inset.

films.[26,27] Therefore, the significant reduction of the 2.9 eV peak intensity after hydrogen plasma treatment, as observed in Fig. 2, suggests a decrease in active Mg acceptor concentration. The fact that the 3.25 eV peak did not completely disappear indicates that some Mg acceptors remained active after the hydrogen plasma treatment. Combining the cross-sectional image and the CL spectra, it can be concluded that the ICP treatment passivated ∼270 nm *p*-GaN near the surface, while the rest of *p*-GaN was not affected.

Figure 3(a) shows a representative *I–V* curve of the MIS junction. The Ohmic contact and the Ni/Au electrode were connected to anode and cathode, respectively, as illustrated in the inset of Fig. 3(a). The junction showed excellent rectifying behaviors at a bias range from −10 V to 10 V, and the reverse leakage current was $\sim 10^{-10}$ A, with on/off ratio at $\sim 10^{7}$. The turn-on voltage, as extracted by linear extrapolation of the slope at the smallest ideality factor point, was ∼1.7 V, which is smaller than that of GaN *p–n* junctions but higher than that of GaN Schottky diodes.[28,29] Figure 3(b) shows the forward I–V characteristics of the devices in a semi-log scale. The minimum ideality factor (n) was ∼1.3, which is comparable to reported as-grown GaN-based junctions.[9,10] In addition, electroluminescence (EL) was also observed at higher forward bias (>3.4 V). The EL spectrum in Fig. 3(c) showed two peaks at 2.25 eV and 2.9 eV. The first was yellow-luminescence (YL) peak due to deep level (DL) transitions. The second peak was at the same position (2.9 eV) as the CL spectrum of untreated p-GaN [Fig. 2(b)]. This indicates that electrons tunnel into *p*-GaN

from the metal/insulator interface at sufficient forward bias, and the 2.9 eV peak is due to the transition from the deep-donor level to the Mg acceptor level.

To understand the electrical properties of the MIS junction, the band diagrams of the MIS structure are schematically shown in Fig. 4. At zero bias, the Fermi level lies around the middle of the *i*-GaN [Fig. 4(a)]. At $V_{bi} > 1.7$ V, the valence band in *p*-GaN moved below the *i*-GaN valence band, and then the holes could be injected form *p*-GaN to *i*-GaN, leading to diffusion current [Fig. 4(c)]. This could illustrate the reason for the unconventional turn-on voltage at 1.7 V [Fig. 3(a), inset]. The hole diffusion current is the main component of the on-current, but the hole concentration in *p*-GaN is limited by Mg activation rate,[30] which could explain the relative high series resistance (~10 kΩ) of the junction. As the forward bias continued to increase over 3.4 V, the electrons could tunnel into *p*-GaN from the metal/insulator interface and relax into the deep donor level. When the tunneled electrons transitioned from the deep donor level to the acceptor level [Fig. 4(d)], blue light (2.9 eV) was emitted, which could explain the EL spectrum in Fig. 3(c). Under a negative bias, due to the hydrogen passivation effect, the *i*-GaN presents very low hole concentration and the current flow is blocked [Fig. 4(b)].

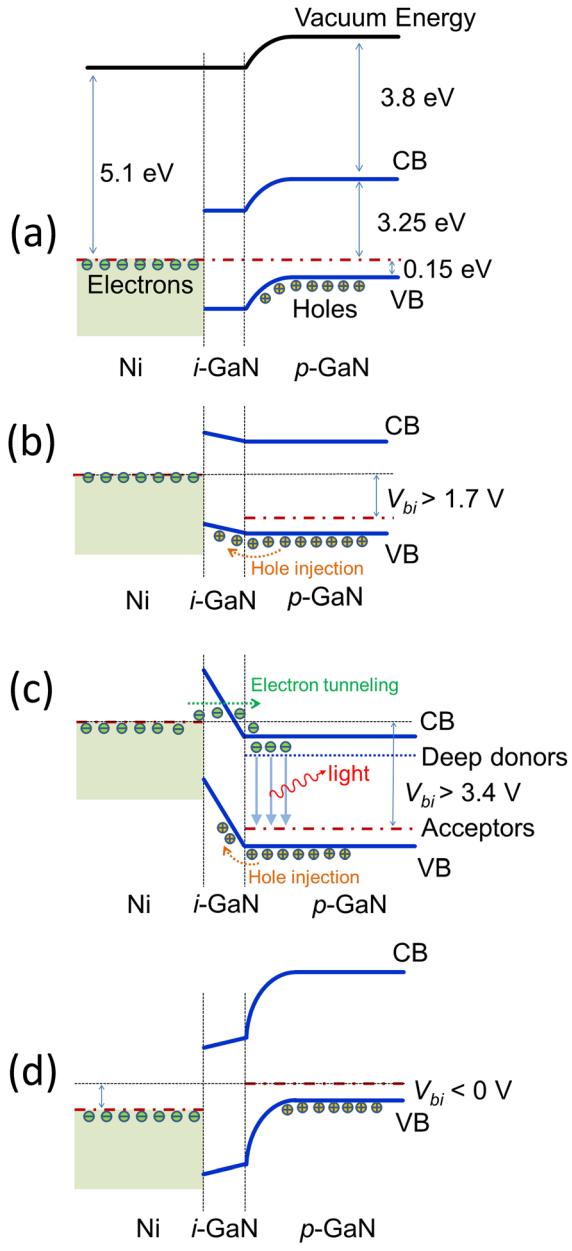

FIG. 4. Band diagram of the MIS device at different biases. (a) At zero bias. (b) At V_{bi} ~1.7 V, holes are injected into *i*-GaN generating a diffusion current. (c) At V_{bi} ~3.4 V, electrons tunnel into *p*-GaN and recombine with holes in *p*-GaN, generating blue emission. (d) At $V_{bi} < 0$ V, the *i*-GaN blocks the current flow.

The thermal stability of the MIS junction was tested by a temperature-dependent *I*–*V* test, shown in Fig. 5(a). The device exhibited good rectifying behaviors even up to 300 °C. The thermal stability can be attributed to strong bonding between hydrogen and Mg in Mg–H complexes.[31,32] The series resistance decreased with the increasing temperature. It is likely because the holes gain higher kinetic energy at higher temperature which leads to a higher level of hole injection and a higher level of on-current. The reverse *I*–*V* curve of the junction is shown in Fig. 5(b). Comparing with reported GaN based MIS junctions with Fe_3O_4,[14] Y_2O_3,[15] Al_2O_3,[16] and Sm_2O_3[17] as the

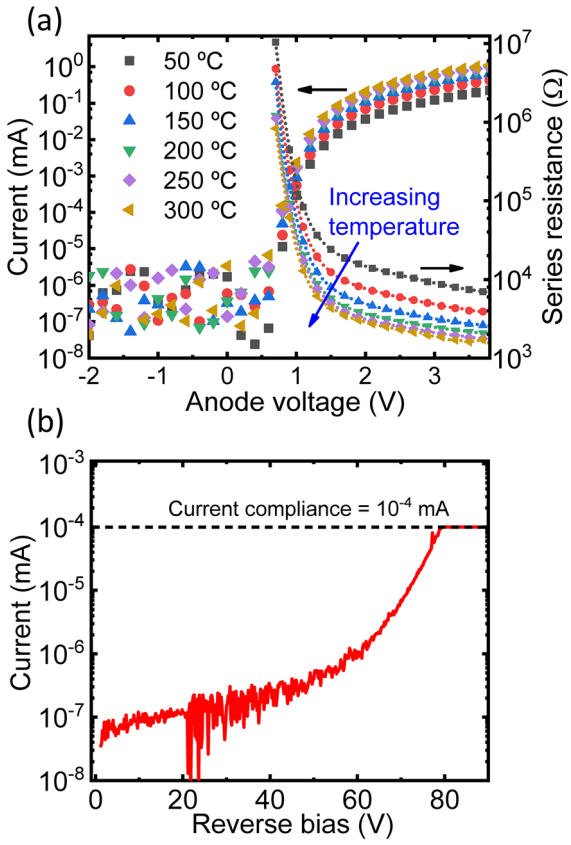

FIG. 5. (a) Temperature dependent *I*–*V* curves from 50 °C to 300 °C. (b) Room temperature reverse *I*–*V* curve.

insulating layer, this device showed excellent electrical performance. The *i*-GaN was fabricated by partially hydrogenating *p*-GaN using low-power plasma. This enabled the ultra-high-quality *i*-GaN/*p*-GaN interface, which can explain the ultra-low reverse leakage. The junction shows soft breakdown with leakage gradually increasing after −60 V. The current compliance was reached at −78 V. The breakdown electric field was calculated to be 2.89 MV/cm, which is comparable to reported breakdown electric fields in avalanche GaN *p*–*n* diodes.[33] The MIS junction has potential applications in ultraviolet (UV) detection,[34] junction termination extension (JTE),[35] and photoelectrochemical (PEC) water splitting.[36]

In summary, we have demonstrated a Ni/*i*-GaN/*p*-GaN MIS junction using a plasma treatment method. The junction was formed by converting part of the as-grown *p*-GaN into *i*-GaN using hydrogen plasma to passivate the acceptors. SEM imaging and CL spectroscopy verified that only ∼270 nm of the *p*-GaN near the surface was passivated. The device shows a turn-on voltage of ∼1.7 V, with excellent rectifying behavior, low leakage, and high temperature stability. This work shows the great potential of incorporating *i*-GaN to fabricate future GaN devices.

This work was supported by the ARPA-E PNDIODES Program monitored by Dr. Isik Kizilyalli and partially supported by the NASA HOTTech Program Grant No. 80NSSC17K0768. The device fabrication was performed at the Center for Solid State Electronics Research at Arizona State University. Access to the NanoFab was supported, in part, by NSF Contract No. ECCS-1542160.

DATA AVAILABILITY

The data that support the findings of this study are available within the article.

REFERENCES

[1]Y. Zhao, R. M. Farrell, Y.-R. Wu, and J. S. Speck, Jpn. J. Appl. Phys., Part 1 **53**, 100206 (2014).
[2]H. Chen, H. Fu, X. Huang, X. Zhang, T.-H. Yang, J. A. Montes, I. Baranowski, and Y. Zhao, Opt. Express **25**, 31758 (2017).
[3]H. Amano, Y. Baines, E. Beam, M. Borga, T. Bouchet, P. R. Chalker, M. Charles, K. J. Chen, N. Chowdhury, R. Chu, C. De Santi, M. M. De Souza, S. Decoutere, L. Di Cioccio, B. Eckardt, T. Egawa, P. Fay, J. J. Freedsman, L. Guido, O. Häberlen, G. Haynes, T. Heckel, D. Hemakumara, P. Houston, J. Hu, M. Hua, Q. Huang, A. Huang, S. Jiang, H. Kawai, D. Kinzer, M. Kuball, A. Kumar, K. B. Lee, X. Li, D. Marcon, M. März, R. McCarthy, G. Meneghesso, M. Meneghini, E. Morvan, A. Nakajima, E. M. S. Narayanan, S. Oliver, T. Palacios, D. Piedra, M. Plissonnier, R. Reddy, M. Sun, I. Thayne, A. Torres, N. Trivellin, V. Unni, M. J. Uren, M. Van Hove, D. J. Wallis, J. Wang, J. Xie, S. Yagi, S. Yang, C. Youtsey, R. Yu, E. Zanoni, S. Zeltner, and Y. Zhang, J. Phys. D **51**, 163001 (2018).
[4]H. Chiu, Y. Chang, B. Li, H. Wang, H. Kao, C. Hu, and R. Xuan, IEEE J. Electron Devices Soc. **6**, 201 (2018).
[5]D. Ji and S. Chowdhury, IEEE Trans. Electron Devices **62**, 3633 (2015).
[6]S. Nakamura, N. Iwasa, M. Senoh, and T. Mukai, Jpn. J. Appl. Phys., Part 1 **31**, 1258 (1992).
[7]W. Li, K. Nomoto, K. Lee, S. M. Islam, Z. Hu, M. Zhu, X. Gao, J. Xie, M. Pilla, D. Jena, and H. G. Xing, Appl. Phys. Lett. **113**, 062105 (2018).
[8]A. Y. Polyakov, N. B. Smirnov, A. V. Govorkov, K. H. Baik, S. J. Pearton, B. Luo, F. Ren, and J. M. Zavada, J. Appl. Phys. **94**, 3960 (2003).
[9]H. Fu, K. Fu, H. Liu, S. R. Alugubelli, X. Huang, H. Chen, J. Montes, T.-H. Yang, C. Yang, J. Zhou, F. A. Ponce, and Y. Zhao, Appl. Phys. Express **12**, 051015 (2019).
[10]H. Fu, K. Fu, X. Huang, H. Chen, I. Baranowski, T. Yang, J. Montes, and Y. Zhao, IEEE Electron Device Lett. **39**, 1018 (2018).
[11]H. Fu, K. Fu, S. R. Alugubelli, C. Cheng, X. Huang, H. Chen, T. Yang, C. Yang, J. Zhou, J. Montes, X. Deng, X. Qi, S. M. Goodnick, F. A. Ponce, and Y. Zhao, IEEE Electron Device Lett. **41**, 127 (2020).
[12]R. Hao, K. Fu, G. Yu, W. Li, J. Yuan, L. Song, Z. Zhang, S. Sun, X. Li, Y. Cai, X. Zhang, and B. Zhang, Appl. Phys. Lett. **109**, 152106 (2016).
[13]R. Hao, C. Sun, B. Fang, N. Xu, Z. Tao, H. Zhang, X. Wei, W. Lin, X. Zhang, G. Yu, Z. Zeng, Y. Cai, X. Zhang, and B. Zhang, Appl. Phys. Express **12**, 036502 (2019).
[14]V. Rajagopal Reddy and C.-J. Choi, Vacuum **164**, 233 (2019).
[15]C. Venkata Prasad, V. Rajagopal Reddy, and C.-J. Choi, Appl. Phys. A **123**, 279 (2017).
[16]K. Čičo, J. Kuzmík, D. Gregušová, R. Stoklas, T. Lalinský, A. Georgakilas, D. Pogany, and K. Fröhlich, Microelectron. Reliab. **47**, 790 (2007).
[17]V. Manjunath, V. Rajagopal Reddy, P. R. Sekhar Reddy, V. Janardhanam, and C.-J. Choi, Curr. Appl. Phys. **17**, 980 (2017).
[18]J. Montes, C. Yang, H. Fu, T.-H. Yang, K. Fu, H. Chen, J. Zhou, X. Huang, and Y. Zhao, Appl. Phys. Lett. **114**, 162103 (2019).
[19]H. Fu, H. Chen, X. Huang, I. Baranowski, J. Montes, T. Yang, and Y. Zhao, IEEE Trans. Electron Devices **65**, 3507 (2018).
[20]S. R. Alugubelli, H. Fu, K. Fu, H. Liu, Y. Zhao, and F. A. Ponce, J. Appl. Phys. **126**, 15704 (2019).
[21]K. Kanaya and S. Okayama, J. Phys. D **5**, 43 (1972).
[22]H. Obloh, K. H. Bachem, U. Kaufmann, M. Kunzer, M. Maier, A. Ramakrishnan, and P. Schlotter, J. Cryst. Growth **195**, 270 (1998).
[23]F. Shahedipour and B. W. Wessels, Appl. Phys. Lett. **76**, 3011 (2000).
[24]U. Kaufmann, M. Kunzer, M. Maier, H. Obloh, A. Ramakrishnan, B. Santic, and P. Schlotter, Appl. Phys. Lett. **72**, 1326 (1998).
[25]H. Amano, J. Electrochem. Soc. **137**, 1639 (1990).
[26]U. Kaufmann, M. Kunzer, H. Obloh, M. Maier, C. Manz, A. Ramakrishnan, and B. Santic, Phys. Rev. B **59**, 5561 (1999).
[27]H. Liu, H. Fu, K. Fu, S. R. Alugubelli, P.-Y. Su, Y. Zhao, and F. A. Ponce, Appl. Phys. Lett. **114**, 082102 (2019).
[28]S. Han, S. Yang, and K. Sheng, IEEE Electron Device Lett. **39**, 572 (2018).
[29]I. C. Kizilyalli, A. P. Edwards, H. Nie, D. Disney, and D. Bour, IEEE Trans. Electron Devices **60**, 3067 (2013).
[30]D.-H. Youn, M. Lachab, M. Hao, T. Sugahara, H. Takenaka, Y. Naoi, and S. Sakai, Jpn. J. Appl. Phys., Part 1 **38**, 631 (1999).
[31]Y. Okamoto, M. Saito, and A. Oshiyama, Jpn. J. Appl. Phys., Part 2 **35**, L807 (1996).
[32]S. Nakamura, T. Mukai, M. Senoh, and N. Iwasa, Jpn. J. Appl. Phys., Part 2 **31**, L139 (1992).
[33]D. Ji, S. Li, B. Ercan, C. Ren, and S. Chowdhury, IEEE Electron Device Lett. **41**, 264 (2020).
[34]X. Sun, D. Li, Z. Li, H. Song, H. Jiang, Y. Chen, G. Miao, and Z. Zhang, Sci. Rep. **5**, 16819 (2015).
[35]M. Shurrab and S. Singh, Semicond. Sci. Technol. **35**, 065005 (2020).
[36]H. Kim, H. Bae, S. W. Bang, S. Kim, S. H. Lee, S.-W. Ryu, and J.-S. Ha, Opt. Express **27**, A206 (2019).